

Electro-mechanical coupling in a one-dimensional model of heart muscle fiber

L. B. Katsnelson*, N. A. Vikulova*, A. G. Kursanov*†, O. E. Solovyova*†, and V. S. Markhasin*†

Abstract — We developed a mathematical model that describes heart muscle fiber as a one-dimensional continuous medium of electrically and mechanically coupled cardiomyocytes through which electrical excitation propagates and initiates muscle contraction. The generic model simulates bilateral relations between the electrical and the mechanical activity of cardiomyocytes in the tissue and accounts for both intracellular and intercellular electro-mechanical couplings and mechano-electric feedback mechanisms.

Keywords: Cardiac mechano-electric feedback, heterogeneous myocardium, mathematical modeling.

Mathematical models are widely used in cardiovascular physiology to describe heart function at different levels of its organization from molecules and cells to the whole organ [1, 8, 16]. Earlier we developed mathematical and experimental models to study the effects of electrical and mechanical interactions arising in myocardial tissue due to regional asynchrony of electrical excitation and mechanical activity [14]. We implemented a so-called muscle duplex approach and discrete chain models, where two or several cardiac muscle segments are connected in-series or in-parallel and interact mechanically with each other [14, 15]. In particular, we showed that the time lag in electrical excitation of muscle segments in such cardiac models resulted in slowly developing gradual changes in their functional characteristics, giving rise to system heterogeneity [11].

The above mathematical models have certain limitations. The most substantial is that the excitation sequence in these models was implemented via pre-described timing of regional stimulation, while electrotonic interactions between cardiomyocytes were not accounted for. So, these models utilized a rather simplified simulation of excitation propagation through the tissue.

To avoid these limitations we developed a continuous one-dimensional (1D)

*Institute of Immunology and Physiology, Ural Branch of the Russian Academy of Sciences, Ekaterinburg 620219, Russia. E-mail: l.katsnelson@iip.uran.ru

†Ural Federal University, Ekaterinburg 620002, Russia

The authors gratefully acknowledge research support from the Russian Foundation for Basic Research (13-04-00365, 14-01-00885, 14-01-31134), from the Ural Branch of the RAS (12-M-14-2009, 12-P-4-1067), Programme No.1 of Basic Research of the Presidium of the RAS, Ural Federal University (No.211 Decree of the Government of Russian Federation of 16th March, 2013).

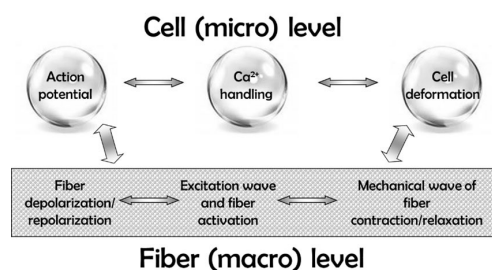


Figure 1. Scheme of electro-mechanical coupling in the myocardium at the cellular level and the tissue level.

mathematical model of the heart muscle fiber as a muscle strand formed of mechanically and electrically interacting cardiomyocytes connected in-series.

The model accounts for both micro- and macrocircuits of the electro-mechanical and mechano-electric interactions in cardiac tissue (Fig. 1). At the cellular level, electro-mechanical coupling (ECC) and mechano-electric feedback (MEF) between the membrane action potential (AP) generation and cellular contraction are provided by the mechano-dependence of intracellular calcium kinetics [15]. The mechanisms of cooperativity in the kinetics of regulatory calcium-troponin complexes and force-generating acto-myosin cross-bridges underlie this mechano-dependence. At the tissue level, electrical waves of depolarization and repolarization and mechanical wave of deformation arising due to the electrical and mechanical coupling between cardiomyocytes also affect each other. ECC and MEF mechanisms in the heart on the cellular level have been widely discussed [10], but the influence of the mechanical interactions between cells on properties of the electrical wave in myocardium remains largely under appreciated.

To assess effects of cardiac MEF by means of 1D modelling, we started with the muscle strand consisting of cardiomyocytes with identical electrical and mechanical properties. In this case we evaluate effects of the initial electrical asynchrony induced by the excitation wave propagation on tissue performance. This is a similar approach to what we used earlier to study effects of cardiac heterogeneity in muscle duplexes and chains of in-series muscle segments [14, 15]. It has been shown that even in the inherently homogeneous cardiac system, the time delays in activation and mechanical interactions between identical muscle segments result in a negative inotropic response and produce gradients of the electro-mechanical characteristics of cardiomyocytes in interacting elements [14]. Now we have a possibility to revise these results by utilizing a more adequate model of cardiac tissue.

1. Mathematical model

We assume a heart muscle fiber as a 1D strand formed of coupled cardiomyocytes. Excitation wave is originated at one edge of the strand and spreads through the cardiomyocytes along the fiber, activating its contraction.

As the size of the cardiomyocytes is sufficiently small compared to the characteristic dimensions of myocardial fibers, any cardiomyocyte of the fiber can be considered as an isopotential point of myocardial tissue [13]. In this case, the fiber may be considered as a continuous 1D medium. On the other hand, each cardiomyocyte of the fiber has its own local, dynamically changing geometry and continuously changes its position in macrospace during the contractile cycle of the fiber. On the macrolevel, local deformations originate the dynamic change in each point (cell) position within the fiber geometry. Thus, an electrical wave of excitation propagates along such a dynamically deformable medium. Therefore, two geometrical spaces are considered in the model:

- (1) microspace representing the cellular geometry;
- (2) macrospace representing the fiber geometry.

In addition, a relationship between these spaces should be defined in the model to determine the mechanical activity of both the fiber and its cells.

Let us consider a 1D muscle strand of a fiber with slack length L and with a single spatial coordinate x varying along the fiber (see Fig. 2). The left boundary of the strand is assigned with the origin $x = 0$, the right boundary has a coordinate $x_F = L$ (see Fig. 2). We assume that the unstretched fiber consists of unstretched cardiomyocytes of identical lengths with a corresponding sarcomere slack length of $1.67 \mu\text{m}$. Thus, each point of the medium is identified by a coordinate $x \{x | x \in [0, x_F]\}$, meaning the distance from the left end of the fiber to this point when the fiber is unstretched and unexcited. The Lagrangian point coordinate does not depend on possible displacements of the material point along the axis during the contractile cycle of the fiber. In other words, if the material point is labeled as x at the slack length state of the fiber, this label will further identify this point (cell) during any fiber deformations.

Electrical and mechanical activity of cells is described by the Ekaterinburg–Oxford mathematical model (EO model) of a single cardiomyocyte [5, 15].

1.1. Cellular mechanics (microlevel)

Figure 2 shows a rheological scheme of a single cardiomyocyte at point x (further, cell x). Active contractile element CE_x is associated with the cardiomyocyte sarcomeres. Sarcomeres generate mechanical force in cell x and cell shortening during auxotonic contractions due to interactions between actin and myosin and cross-bridges formation. This occurs in consequence of calcium binding to the regulatory protein troponin C (CaTnC complexes). Detailed interactions between these molecular processes are described in our previous papers [3, 6]; the full list of equations is presented at a CellML repository (see <http://models.cellml.org/e/b9/>).

Suppose $l_1(x, t)$ is the relative change in the length of CE_x the cell x against its slack length (normalized by the sarcomere slack length of $1.67 \mu\text{m}$). The force generated by CE_x is defined in the model as

$$F_{CE_x} = F_{CE}(x, t) = \lambda(x) N(x, t) p(x, \dot{l}_1(x, t)) \quad (1.1)$$

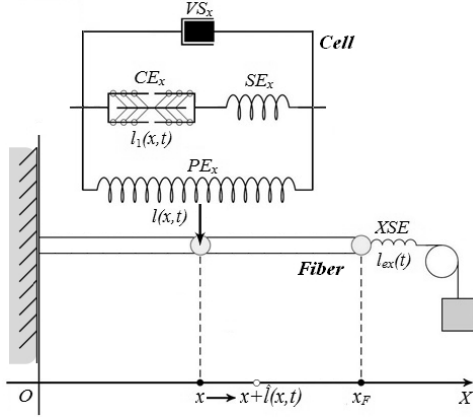


Figure 2. Scheme of a 1D heart muscle strand. The rheological scheme shows a model of a single cardiomyocyte of coordinate x , where a contractile element (CE_x) is connected to in-series and parallel passive elastic elements (SE_x , PE_x), and a viscous element (VS_x) is in-parallel to PE_x . XSE is an external in-series elastic element. Variables $l(x,t)$, $l_1(x,t)$, $l_{ex}(t)$ define deformations of PE_x , CE_x , and XSE , respectively, relative to their slack lengths.

where $p(x, \dot{l}_1(x,t))$ is an explicit function that specifies the average force developed by a cross-bridge depending on $\dot{l}_1(x,t)$, which is the velocity of CE_x shortening/stretching; $N(x,t)$ is the concentration of force-generating cross-bridges in CE_x ; $\lambda(x)$ is a scale coefficient.

Further, we often skip coordinate x for intracellular variables and coefficients, keeping in mind that each cell x in the fiber may have its own set of coefficient values.

Cross-bridge concentration $N(t)$ in cell x at moment t results from the kinetics of cross-bridges attachment/detachment. Concentration $N(t)$ not only directly affects mechanical behaviour of the contractile element but the cross-bridge kinetics depends on the mechanical conditions as follows:

$$\frac{dN}{dt} = k_+([\text{Ca}_{\text{TnC}}], l_1, \dot{l}_1) (1 - N) - k_-(\dot{l}_1) N \quad (1.2)$$

where $k_+([\text{Ca}_{\text{TnC}}], l_1, \dot{l}_1)$ and $k_-(\dot{l}_1)$ are the on- and off-rate ‘constants’, respectively, of force-generating cross-bridges cycling. This kinetics depends non-linearly on the concentration of CaTnC complexes ($[\text{Ca}_{\text{TnC}}](t)$) and on both the length of CE_x and on the velocity of its deformation (i.e., on the variables $l_1(t)$ and $\dot{l}_1(t)$).

The kinetics of $[\text{Ca}_{\text{TnC}}]$ is described by the equation

$$\frac{d[\text{Ca}_{\text{TnC}}]}{dt} = k_{\text{on}} \cdot ([\text{Ca}_{\text{TnC}}]_{\text{tot}} - [\text{Ca}_{\text{TnC}}]) \cdot [\text{Ca}^{2+}]_i - k_{\text{off}}(N, [\text{Ca}_{\text{TnC}}]) \cdot [\text{Ca}_{\text{TnC}}] \quad (1.3)$$

where $[\text{Ca}^{2+}]_i(t)$ is the intracellular Ca^{2+} concentration; k_{on} is the rate constant of CaTnC association, $k_{\text{off}}(N, [\text{Ca}_{\text{TnC}}])$ is the rate ‘constant’ of CaTnC dissociation,

which is a function of the mechanical state of the contractile element (variable $N(t)$) and calcium kinetics ($[Ca_{TnC}](t)$).

This highly non-linear functional dependence of k_{off} on the current state of sarcomere activity reflects mechanisms of cooperative calcium activation of the contractile proteins: the affinity of troponin C for Ca^{2+} increases (k_{off} decreases) with an increase in (a) the fraction of force-generating cross-bridges $N(t)$ and (b) $[Ca_{TnC}](t)$. Mechano-dependent cross-bridges kinetics affect the CaTnC kinetics and thereby the Ca^{2+} kinetics, i.e., both become mechano-sensitive. Cooperative mechanisms of CaTnC kinetics as well as respective equations are identified and justified in our previous papers [3, 5, 15].

Thus, direct links and feedback between Ca^{2+} kinetics, CE_x deformations, and force generation are defined in the EO model and ensured from the cooperative mechanisms of myofilament Ca^{2+} activation.

Besides the active contractile element CE_x , in the rheological scheme of cardiomyocyte x there are also elastic and viscous elements (SE_x , PE_x and VS_x , see Fig. 2), which mainly determine mechanical properties of passive myocardium but also may modulate the active myocardial mechanics [5].

Suppose $l(x, t)$ is a relative change in the cell x length per sarcomere (normalized by its sarcomere slack length). In correspondence with the rheological scheme, $l(x, t)$ coincides with the deviation of the length of the parallel elastic element PE_x from its slack length.

The forces generated by SE_x and PE_x are defined as follows:

$$F_{SE_x} = F_{SE}(x, t) = \beta_1 (e^{\alpha_1(l(t)-l_1(t))} - 1) \quad (1.4)$$

$$F_{PE_x} = F_{PE}(x, t) = \beta_2 (e^{\alpha_2 \cdot l(t)} - 1) \quad (1.5)$$

with parameters α_1 , β_1 , α_2 , and β_2 justified in our previous works.

The viscosity coefficient of the damper VS_x in the rheological scheme of the cardiomyocyte is considered to be dependent on the degree of stretching the cell [5]. The damper VS_x , being parallel to PE_x (and the entire length of $CE_x + SE_x$), generates a force proportional to the velocity of the cell shortening $\dot{l}(t)$:

$$\begin{aligned} F_{VS_x} &= F_{VS}(x, t) = k_{\text{vis}} \dot{l}(t) \\ k_{\text{vis}} &= \beta_v e^{\alpha_v \cdot l(t)} \end{aligned} \quad (1.6)$$

where k_{vis} is the length-dependent viscosity coefficient for VS_x [5].

The following equations define the force F_x that is developed by cardiomyocyte at point x :

$$\begin{aligned} F_x &= F_{CE_x} + F_{PE_x} + F_{VS_x} \\ F_{CE_x} &= F_{SE_x}. \end{aligned} \quad (1.7)$$

1.2. Fiber mechanics (macrolevel)

Let $\hat{l}(x, t)$ define a deviation of cell x from its reference position in the unstretched and unexcited fiber. Therefore, the current time-dependent position of the cell x at a given moment during the contractile cycle is $\hat{x} = x + \hat{l}(x, t)$.

An external serial elastic element XSE is introduced in the rheological scheme of the fiber macromodel (Fig. 2). It allows us to reproduce experiments on multicellular muscle strips and accounts for a compliance in the area of the cut muscle edge, which is bound to a servomotor arm [5].

Let $l_{\text{ex}}(t)$ be a deviation of XSE length from its slack length. The force generated by XSE is defined as follows:

$$F_{XSE} = F_{XSE}(t) = \beta_3 (e^{\alpha_3 l_{\text{ex}}(t)} - 1) \quad (1.8)$$

where α_3 and β_3 are model parameters.

Kinematic conditions of the in-series connection between the cells in the fiber suggest that the force F_x generated by each cell x is equal to the force of any other cell in the strand and equal to the force of XSE :

$$F_x = F_{XSE}. \quad (1.9)$$

Additional conditions completing F_x determination are governed by the mode of the fiber contraction.

The *isometric contraction* is characterized by a fixed length of the fiber during the contractile cycle. Let $l_m(t)$ be a fiber deformation against its slack length. It is determined by the initial fiber prestretch due to an applied preload ρ and remains constant during the entire isometric contraction/relaxation. In the isometric mode, a displacement of the right end of the fiber $\hat{l}(x_F, t)$ during an active contraction is balanced by stretching the external passive-elastic element XSE so that the sum of their deformations remains constant:

$$l_m(t) = \hat{l}(x_F, t) + l_{\text{ex}}(t) \equiv \text{const}. \quad (1.10)$$

In the *isotonic mode* of the fiber contraction, the fiber undergoes active shortening/lengthening under a fixed afterload $\bar{F} \equiv \text{const}$. In this case the overall fiber force, each cell force, and XSE force are equal to each other and to this afterload:

$$F_x = F_{XSE} = \bar{F}. \quad (1.11)$$

Thus, dynamics of $\hat{l}(x, t)$ and $l_{\text{ex}}(t)$ describe the macroscopic mechanics of the fiber.

1.3. Micro- and macromechanics coupling

The specific feature of a continuous model of muscle mechanics is a combination of the global deformations of the fiber and the local geometry of its cells. We suggest

a displacement $\hat{l}(x,t)$ of point x from its reference position in the unloaded fiber to be an integral of the relative changes in the cell lengths over the fiber segment $[0,x]$ at time t :

$$\hat{l}(x,t) = \int_0^x l(\xi,t) d\xi. \quad (1.12)$$

In other words, the local deformation of the fiber at the point x in macrospace is equal to the relative deformation of the cell x in microspace:

$$\frac{\partial \hat{l}(x,t)}{\partial x} = l(x,t). \quad (1.13)$$

The above equations govern the coupling between micro- and macromechanics in the model.

Thus, during the propagation of the electrical signal from the left to the right end of the fiber, the lengths of all contracting cells continuously change, providing for the global deformation of the fiber and overall force generation.

The boundary conditions (at $x = 0$ and $x = x_F$) for equation (1.12) during isometric contractions is given by equation (1.10):

$$\hat{l}(0,t) = 0 \quad (1.14)$$

$$\hat{l}(x_F,t) + l_{ex}(t) \equiv \hat{l}(x_F,0) + l_{ex}(0). \quad (1.15)$$

The initial conditions at $t = 0$ for $\hat{l}(x,0)$ and $l_{ex}(0)$ arise from the equations (1.7), (1.11) with a preload ρ applied to the fiber and prestretching it up to the value $l_m(0)$ over the slack length.

Similarly, in the isotonic mode of contraction, fiber deformations $\hat{l}(x_F,t)$ and $l_{ex}(t)$ are determined from the equations (1.7), (1.11) for a given afterload \bar{F} .

1.4. Micro- and macroelectrical coupling

The mathematical description of the dynamics of membrane potential and ionic currents in an individual cell x is inherited from the cellular EO model [15]. The characteristics of the depolarization and repolarization waves determine the macroscopic electrophysiology of the fiber.

Let the excitation wave propagate from the left fiber end ($x = 0$) towards the right end ($x = x_F$).

Let us start with the assumption that positions of material points in the 1D fiber model do not change during the contraction-relaxation cycle. Note that such a static model is a widely used simplification in electrophysiological mathematical modelling. In this case, the electrical excitation of the fiber is governed by the cable reaction-diffusion equation [7] for the membrane potential $V(x,t)$ in the cell x at time t :

$$\frac{\partial V(x,t)}{\partial t} = D \frac{\partial^2 V(x,t)}{\partial x^2} - \frac{1}{C_m(x)} \sum i_{ion}(x,t) \quad (1.16)$$

where $C_m(x)$ denotes the membrane capacity of the cell x and D is the conductivity coefficient, which determines the velocity of excitation propagation along the fiber. The coefficient D is also conventionally called a diffusion coefficient of the equation (1.16).

The first term of the equation determines the excitation spread through diffusively coupled cells along the fiber (macrolevel), and the second term describes change in membrane potential $V(x, t)$ in the cell x due to local transmembrane ionic currents $i_{\text{ion}}(x, t)$ in this cell (microlevel).

However, if the mechanical activity is taken into consideration in the fiber model, it should account for the fact that the position of the cell x in the physical space is inevitably shifted from the reference slack position x due to the initial fiber prestretching and further contraction-relaxation movements. Therefore, the electrical signal propagating through the cell x finds it in the other position of the macrospace.

Let the cell x (material point) move to point $\hat{x} = x + \hat{l}(x, t)$, where $\hat{l}(x, t)$ is the deviation of the point x from the reference coordinate.

In this case, the diffusion term in equation (1.16) has to be calculated relatively to the point \hat{x} as $D\partial^2V/\partial\hat{x}^2$ as follows:

$$\frac{\partial V}{\partial \hat{x}} = \frac{\partial V}{\partial x} \frac{\partial x}{\partial \hat{x}} = \frac{\partial V}{\partial x} \frac{1}{1+l(x,t)}.$$

Here, we used equation (1.13) for the coupling between the local deformation of the fiber and relative deformation of the cell x :

$$\begin{aligned} \frac{\partial \hat{x}}{\partial x} &= \frac{\partial(x + \hat{l}(x, t))}{\partial x} = 1 + l(x, t) \\ \frac{\partial^2 V}{\partial \hat{x}^2} &= \frac{\frac{\partial}{\partial \hat{x}} \left(\frac{\partial V}{\partial x} \right) (1 + l(x, t)) - \frac{\partial V}{\partial x} \cdot \frac{\partial l(x, t)}{\partial \hat{x}}}{(1 + l(x, t))^2} = [\dots] = \frac{\frac{\partial^2 V}{\partial x^2} \cdot (1 + l(x, t)) - l'_x(x, t) \cdot \frac{\partial V}{\partial x}}{(1 + l(x, t))^3}. \end{aligned}$$

Accordingly, we come to the following modified equation:

$$\frac{\partial V}{\partial t} = D \cdot \frac{\frac{\partial^2 V}{\partial x^2} \cdot (1 + l(x, t)) - l'_x(x, t) \cdot \frac{\partial V}{\partial x}}{(1 + l(x, t))^3} - \frac{1}{C_m(x)} \cdot \sum i_{\text{ion}}(x, t). \quad (1.17)$$

Note that the macro-level diffusional term of equation (1.17) now contains the mechanical phase variable $l(x, t)$ of the cellular microlevel.

Boundary conditions for the problem (1.17) are set as follows:

- (1) A short-term stimulating depolarizing current $i_{\text{stim}}(t) = -3 \text{ nA}$ is applied for 2–3 ms (inherited from Noble'98 model [12]) at the left end of the fiber (at point $x = 0$), initiating excitation in the boundary cell. Then, the boundary value for $V(0, t)$ is calculated from the ordinary differential equation (ODE)

of the cellular EO model taking into account the mechanical interactions with neighbour cells but ignoring the electrical influence from the right adjacent cells: $V(0, t) = V_{\text{ODE}}(t)$.

Depolarization of the membrane in all other cells is initiated by the electrical wave propagation from cell to cell without any additional stimulating trans-membrane currents.

- (2) The right end of the fiber ($x = x_F$) is assumed to be electrically isolated, i.e., there are no ionic currents through the boundary point:

$$\frac{\partial V(x_F, t)}{\partial x} = 0.$$

A resting potential value is used for all fiber cells as initial conditions at $t = 0$, which is the same as in the EO model:

$$V(x, 0) = V_{\text{rest}}(x).$$

Thus, the model equations define mechanisms of electro-mechanical coupling and mechano-electric feedback both at the cellular level (via mechano-dependence of Ca^{2+} kinetics, which contributes to the time course of Ca^{2+} -dependent ionic currents) and at the fiber level (via length-dependence of the diffusion component of the modified cable equation).

Several functional parameters were calculated to characterize the electrical wave. An average velocity of the depolarization wave V_{dw} along the fiber was calculated as the ratio of the initial fiber length to the propagating time Δt_{dep} from the left to the right end of the fiber. The latter was also called as the dispersion of depolarization $DD = \Delta t_{\text{dep}}$ throughout the strand. The dispersion of repolarization $DR = \Delta t_{\text{rep}}$ in the strand was calculated as the difference between the time to reach 90% of repolarization in the fiber ends. The average velocity of the repolarization wave V_{rw} was characterized by the ratio of the initial fiber length and Δt_{rep} .

1.5. Numerical methods

We used a method of splitting [4] to solve the boundary problem for equation (1.17).

During each discrete time interval Δt , first we calculated the membrane potential in each point x from the non-linear ordinary differential equation:

$$\frac{dV(x, t)}{dt} = -\frac{1}{C_m(x)} \sum i_{\text{ion}}(x, t)$$

using explicit Euler or Runge–Kutta methods.

Then we used these values as initial values to solve the linear diffusion equation with corresponding boundary conditions for the same time step Δt :

$$\frac{\partial V}{\partial t} = D \frac{\frac{\partial^2 V}{\partial x^2} (1 + l(x, t)) - l'_x(x, t) \frac{\partial V}{\partial x}}{(1 + l(x, t))^3}.$$

A stable implicit difference scheme was built to solve the problem. The equations were discretized with a time step of $\Delta t = 10^{-5}$ s and a spacial step of $\Delta x = 0.25$ mm. This gives a system of linear algebraic equations with a tridiagonal matrix for numerical values V_i^j for action potential $V(x, t)$ at point x_i at time t_j . The linear system was solved by a tridiagonal matrix algorithm.

The mechanical block of the model was solved in the same discretization nodes. Macrovariables $\hat{l}(x_i, t_j)$ and $l_{\text{ex}}(t_j)$ were calculated by numerical solution of equations (1.7), (1.9) in parallel with numerical integration of (1.12) with consistent boundary conditions (1.10) or (1.11). Cellular mechanics was calculated together with ionic concentrations and membrane potential at each discrete point x_i by numerical integration of the corresponding cellular EO model.

2. Numerical simulations

Figures 3 and 4 illustrate results of numerical simulations of the electrical and mechanical activity of contracting myocardial strand produced by the created 1D electro-mechanical model (EMM) consisting of identical virtual cells. The data are derived from the steady-state twitches of the strand of a fixed 50.5 mm length (26 in every cell) in the isometric mode of contraction with stimulation frequency of 1 Hz.

Presented data reveal essential gradients in both electrical and mechanical activity of coupled cells along the strand, which was originated from the excitation wave spread and both intra- and inter-cellular mechano-electrical coupling in myocardial tissue. The electrical and mechanical gradients turned out to be dependent on the conduction velocity (diffusion coefficient D) in the tissue.

The data calculated for various values of the diffusion coefficient D are shown in the figures in comparison with each other and with the reference model (RM). The latter simulates purely homogeneous strand with simultaneous excitation of identical cells. Electrical and mechanical asynchrony are excluded, and any factors of cellular interaction are totally eliminated in the RM. Therefore contracting cells in the RM behave exactly like isolated cardiomyocytes in the isometric contraction mode.

The results of simulations demonstrate essential effects of cell coupling in the tissue on their electrical and mechanical activity as compared with isolated cells. The effects of asynchronous excitation on the strand function increase with a decrease in the conduction velocity in the tissue.

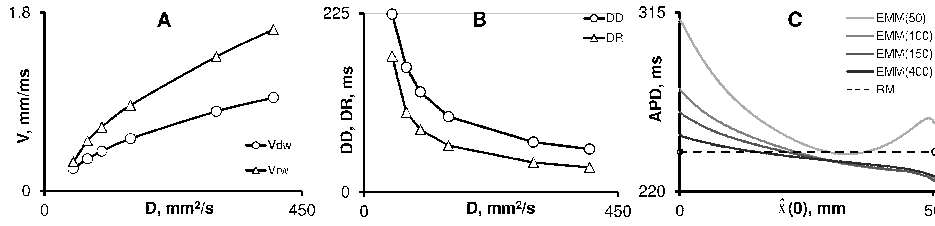


Figure 3. Characteristics of the electrical waves in the 1D electro-mechanical model (EMM) of the muscle fibre. (A) Dependence of the velocity of depolarization wave (V_{dw}) and the velocity of repolarization wave (V_{rw}) on the diffusion coefficient D . (B) Dependence of the dispersion of depolarization (DD) and the dispersion of repolarization (DR) on the diffusion coefficient D . (C) Distribution of action potential duration (APD) along the strand in EMM at various diffusion coefficients ($D = 50, 100, 150, 400 \text{ mm}^2/\text{s}$) against the reference model (RM, dashed line).

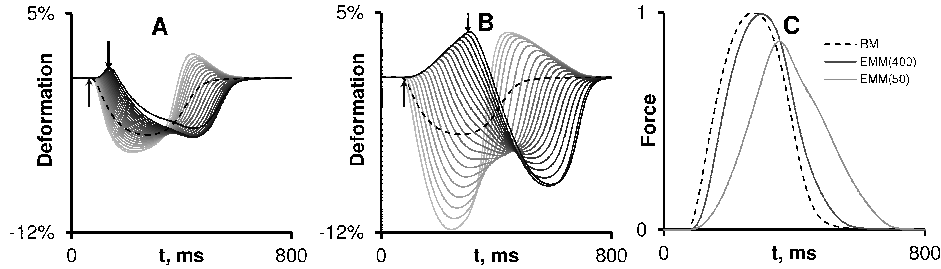


Figure 4. Mechanical activity in the EMM at various diffusion coefficients. (A), (B) Time course of cellular deformations (expressed as % of initial cell length) along the fiber at high (A, $D = 400 \text{ mm}^2/\text{s}$) and low (B, $D = 50 \text{ mm}^2/\text{s}$) conduction velocity. Excitation onsets in the border cells are shown by up and down arrows, respectively. Dashed line shows cell deformation in the reference model (RM). (C) Force generated by the EMM (solid lines) in the case of (A) and (B) against the isometric contraction of the RM (dashed line). Force is normalized to the peak force in the RM.

3. Conclusion

Mathematical models in cardiac physiology are widely used but they often do not give an entire picture of mechanisms underlying electro-mechanical behaviour of myocardium. We have developed a mathematical model of the heart muscle fiber, describing both electrical excitation propagation and contraction in myocardial strand. The main advantage of the 1D model is the integration of cardiac excitation-contraction coupling and mechano-electric feedback mechanisms at both the cellular and the tissue levels.

The model predictions suggest that a decrease in the conduction velocity (a decrease in the diffusion coefficient D) in the fiber causes much steeper decrease in the velocity of the repolarization wave, and an increase in dispersion of repolarization producing a substrate for arrhythmia (see Fig. 3). Moreover, an increase in the asynchrony of regional mechanical activation caused by the slowing down of excitation spread, increases local cell deformations and has a negative effect on fiber contractility slowing down both contraction and relaxation and decreasing maximal force production (see Fig. 4).

Model analysis allows us to reveal cellular mechanisms underlying the macroscopic effects of electro-mechanical coupling in myocardium. Mechanical interactions of the asynchronously activated cells evolve dynamic strain fields in the tissue (see Fig. 4). This via cooperativity mechanisms affects mechano-dependent calcium activation of myofilaments in the cells, and therefore modulates intracellular calcium kinetics and action potential generation (see Fig. 3). Therefore, mechanical wave affects the electrical wave of repolarization and decreases dispersion of repolarization against dispersion of depolarization in the fiber (compare DR and DD for each given value of D in Fig. 3).

In this study we have tried to integrate important pathways of regulation of myocardium contraction involving various intracellular and inter-cellular mechano-electric feedbacks. Of course, the feedback loop in the present model is far from comprehensive, as it also is known to include contributions from several other directly mechano-dependent mechanisms on the cellular and tissue levels. Some of them are worth special mentioning.

- On the intracellular level, there are stretch-activated ion channels in the sarcolemma and intracellular mechano-dependent membrane systems including Ca^{2+} stores [2, 9].
- On the tissue level, there is a length-dependence of the cell conductivity (a length-dependence of the diffusion coefficient D), which should account for dynamic change in the cross-section of cells at their constant volume.

We are going to introduce the above mechanisms in the tissue model later on and assess their contributions to the electrical and mechanical performance of the heart muscle.

References

1. R. H. Clayton, O. Bernus, E. M. Cherry, H. Dierckx, F. H. Fenton, L. Mirabella, A. V. Panfilov, F. B. Sachse, G. Seemann, and H. Zhang, Models of cardiac tissue electrophysiology: progress, challenges and open questions. *Prog. Biophys. Mol. Biol.* **104** (2011), No. 1–3, 22–48.
2. G. Iribe, C. W. Ward, P. Camelliti, C. Bollensdorff, F. Mason, R. A. Burton, A. Garny, M. K. Morphew, A. Hoenger, W. J. Lederer, and P. Kohl, Axial stretch of rat single ventricular cardiomyocytes causes an acute and transient increase in Ca^{2+} spark rate. *Circ. Res.* **104** (2009), 787–795.
3. V. Izakov, L. B. Katsnelson, F. A. Blyakhman, V. S. Markhasin, and T. F. Shklyar, Cooperative effects due to calcium binding by troponin and their consequences for contraction and relaxation of cardiac muscle under various conditions of mechanical loading. *Circ. Res.* **69** (1991), No. 5, 1171–1184.
4. T. Jahnke and C. Lubich, Error bounds for exponential operator splittings. *BIT Numer. Math.* **40** (2000), No. 4, 735–744.
5. L. B. Katsnelson, T. Sulman, O. Solovyova, and V. S. Markhasin, Role of myocardial viscoelasticity in disturbances of electrical and mechanical activity in calcium overloaded cardiomyocytes: mathematical modelling. *J. Theor. Biol.* **272** (2011), No. 1, 83–95.

6. L. B. Katsnelson, T. B. Sulman, O. E. Solovyova, and V. S. Markhasin, Cooperative mechanisms of thin filament activation and their contribution to the myocardial contractile function. Assessment in a mathematical model. *Biophys.* **54** (2009), No. 1, 39–46.
7. J. P. Keener and J. Sneyd, *Mathematical Physiology: I: Cellular Physiology*. Springer, 2008.
8. R. C. P. Kerckhoffs, S. N. Healy, T. P. Usyk, and A. D. McCulloch, Computational methods for cardiac electromechanics. *Proceedings of the IEEE* **94** (2006), No. 4, 769–782.
9. P. Kohl, C. Bollensdorff, and A. Garny, Effects of mechanosensitive ion channels on ventricular electrophysiology: experimental and theoretical models. *Exp. Physiol.* **91** (2006), 307–321.
10. P. Kohl, F. Sachs, and M. R. Franz, *Cardiac mechano-electric coupling and arrhythmias*. OUP Oxford, 2011.
11. V. S. Markhasin, A. A. Balakin, L. B. Katsnelson, P. Kononov, O. N. Lookin, Y. Protsenko, and O. Solovyova, Slow force response and auto-regulation of contractility in heterogeneous myocardium. *Prog. Biophys. Mol. Biol.* **110** (2012), No. 2–3, 305–318.
12. D. Noble, A. Varghese, P. Kohl, and P. Noble, Improved guinea-pig ventricular cell model incorporating a diadic space, I_{Kr} and I_{Ks} , and length- and tension-dependent processes. *Can. J. Cardiol.* **14** (1998), No. 1, 123–134.
13. R. M. Shaw and Y. Rudy, Ionic mechanisms of propagation in cardiac tissue. Roles of the sodium and L-type calcium currents during reduced excitability and decreased gap junction coupling. *Circ. Res.* **81** (1997), No. 5, 727–741.
14. O. Solovyova, L. B. Katsnelson, P. Kononov, O. Lookin, A. S. Moskvina, Y. L. Protsenko, N. Vikulova, P. Kohl, and V. S. Markhasin, Activation sequence as a key factor in spatio-temporal optimization of myocardial function. *Philos. Transact. A Math. Phys. Eng. Sci.* **364** (2006), No. 1843, 1367–1383.
15. O. Solovyova, N. Vikulova, L. B. Katsnelson, V. S. Markhasin, P. J. Noble, A. Garny, P. Kohl, and D. Noble, Mechanical interaction of heterogeneous cardiac muscle segments in silico: effects on Ca^{2+} handling and action potential. *IJBC* **13** (2003), No. 12, 3757–3782.
16. N. A. Trayanova, Whole-heart modelling: applications to cardiac electrophysiology and electromechanics. *Circ. Res.* **108** (2011), No. 1, 113–128.